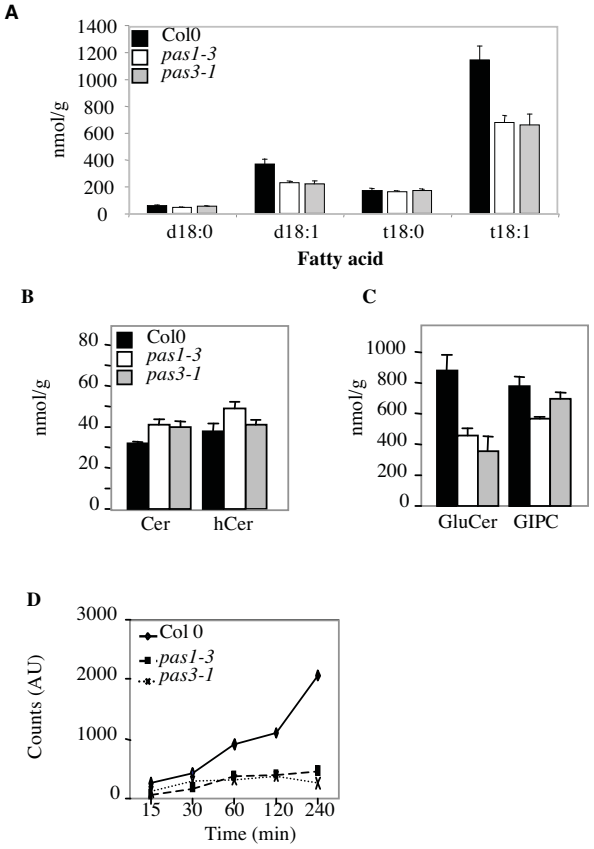

Supplemental Figure 1 . VLCFAs and sphingolipids biosynthesis are altered in *pas1-3* and *pas3-1* mutants.

(A) Long Chain base composition in total sphingolipids of *pas1-3* and *pas3-1* mutants.

(B - C) Ceramides (Cer), hydroxyceramides (hCer) (A) and Glucosylceramides (GluCer), Glycosylinositolphosphoceramides (GIPC) (B) composition in wild-type (Col0, black bars), *pas1-3* (white bars) and *pas3-1* (grey bars) seedlings.

(D) GluCer synthesis in wild-type (Col0), *pas1-3* and *pas3-1* mutants. Glucer synthesis was analyzed after ^{14}C-acetate pulse labeling during the time indicated.

Data represents the mean of 3 independent analyses except for (D) where a representative experiment is shown. Error bar is SEM.

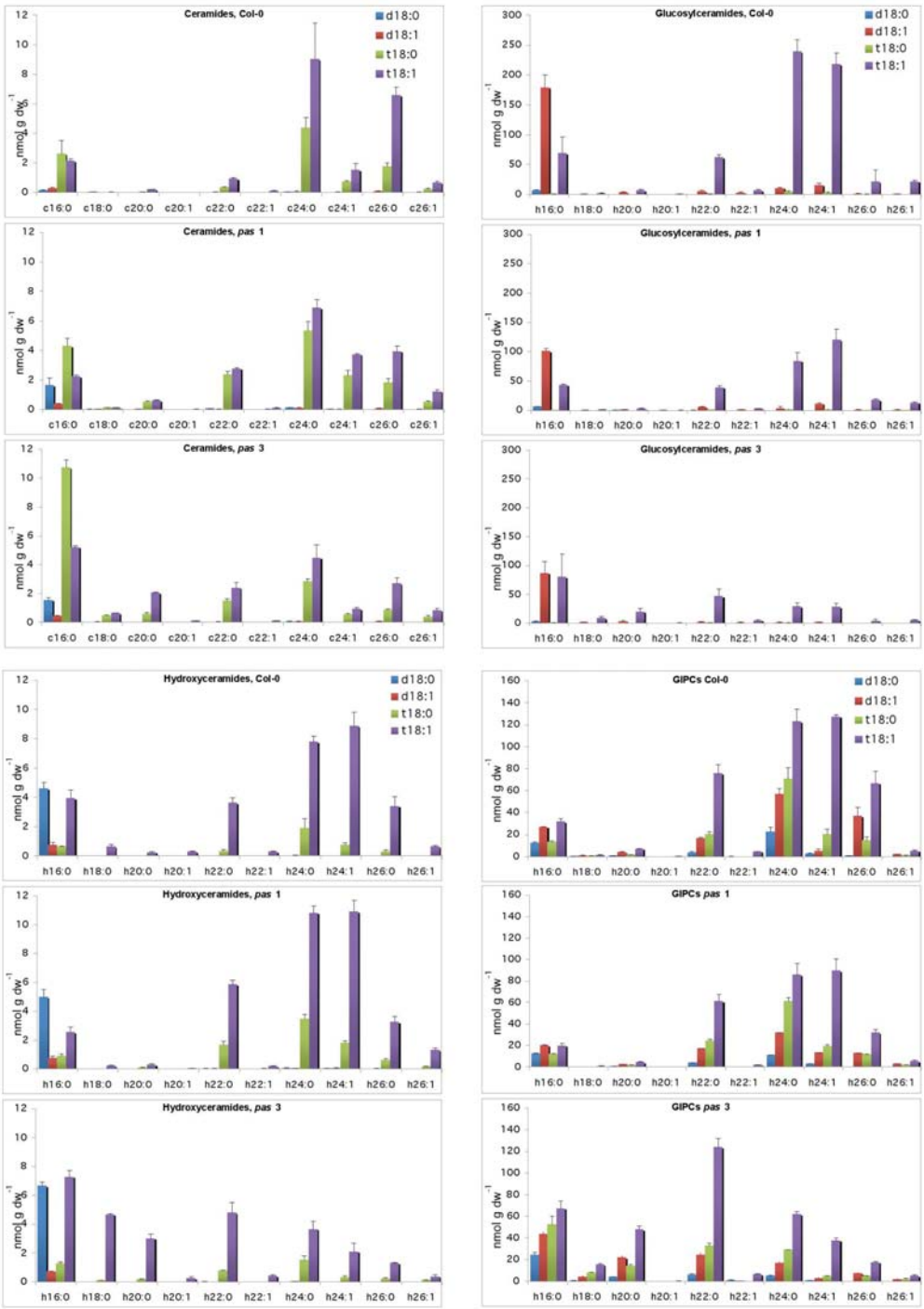

Supplemental Figure 2. Ceramides, hydroxyceramides, Glucosylceramides and Glycosylinositolphosphorylceramides (GIPCs) composition of *pas1-3* (*pas1*) and *pas3-1* (*pas3*) mutants. The level of each sphingolipid was analyzed from wild-type, *pas1-3* and *pas3-1* seedlings and separated according to their fatty acyl length (labelled c for ceramides and h for hydroxyceramides, Glucer and GIPC since they are hydroxylated) and the nature of the Long Chain Base (LCB) moiety (d18:0, d18:1, t18:0, t18:1). Results are the mean of three independent experiments; error bar is SEM.

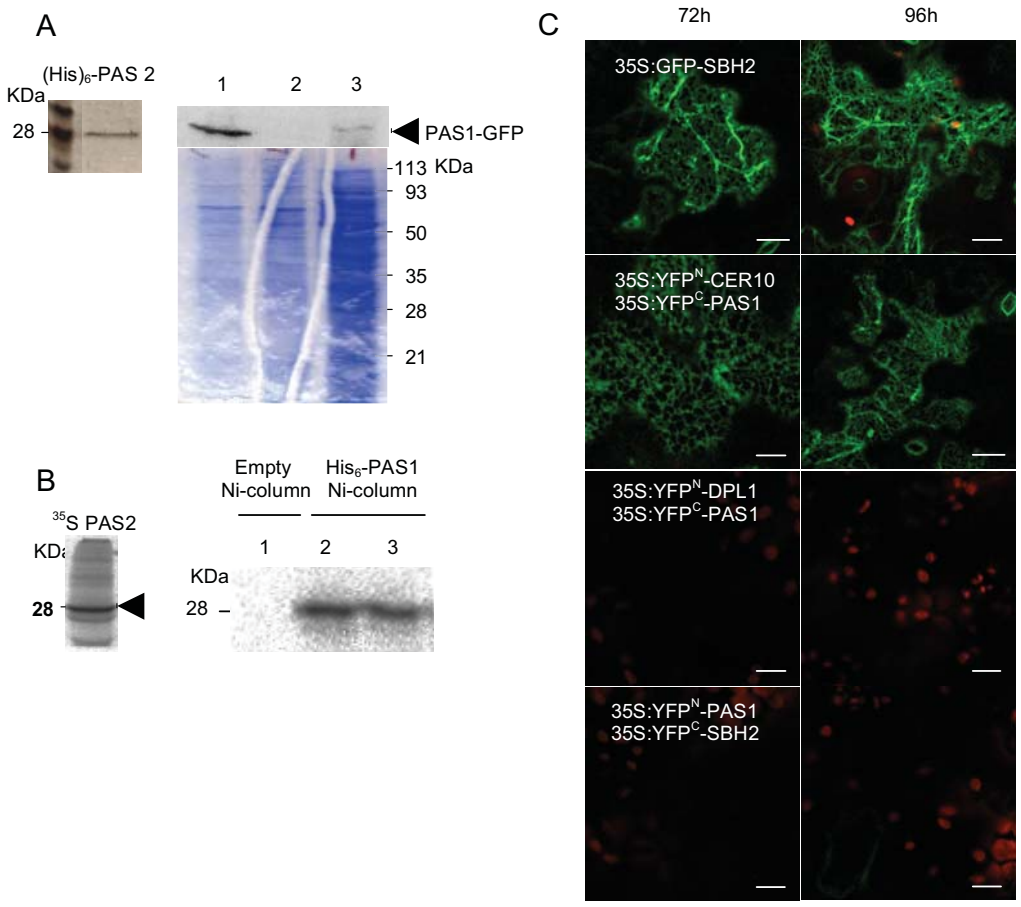

Supplemental Figure 3: PAS1 interacts with elongase enzymes.

(A) The histidine tagged PAS2 protein (His_6-PAS2) was produced in the Rapid Translation System cell free system (RTS, Roche Inc). Expression of tagged PAS2 protein was monitored by silver staining of a SDS-PAGE (left) and used to prepare an affinity Ni-based affinity column (His_6-PAS2). Total extract was prepared from several grams of cells that were ground in liquid nitrogen and 1– 4 mg/ml protein was extracted in extraction buffer (60 mM Tris, pH 6.8, 20% glycerol, 10 mM dithiothreitol, 0.1% Triton, and protease inhibitors). Protein extract from BY2 cells expressing 35S: PAS1-GFP (3) was used to load a Ni PAS2 column (1), or an empty Ni column (2). After washing, proteins were eluted and analyzed by western blot with an anti GFP antibody (Roche Applied Science) (right top). Proteins from the eluates of both columns (1 and 2) as well as total extract (3) were also coomassie stained (right below). The transgenic BY2 cell line expressing 35S: PAS1-GFP was described previously (Smyczynski et al. 2006). The *in vitro* pull-down using recombinant Ni-PAS2 affinity column was performed according to Da Costa et al. 2006.

(B) Radiolabelled PAS2 was produced in RTS like in (A) except that synthesis was performed in presence of ^{35}S-methionine. ^{35}S-PAS2 synthesis was monitored by autoradiography of a SDS-PAGE (left). ^{35}S-PAS2 was loaded on an empty Ni-Column (1) or two independent His_6-PAS1 Ni-columns (2, 3). The *in vitro* pull-down was performed like in (A).

(C) PAS1 interacts specifically with CER10 72 (left) and 96h (right) after transformation. Expression of *35S:GFP-SBH2, 35S:YFP^N-CER10/35S:YFP^C-PAS1, 35S:YFP^N-PAS1/35S:DPL1-YFP^C, 35SYFP^N-PAS1/35S:YFP^C-SBH2* in Arabidopsis epidermal cotyledon cells. Red signal is the plastid autofluorescence. Bars are 10μm.

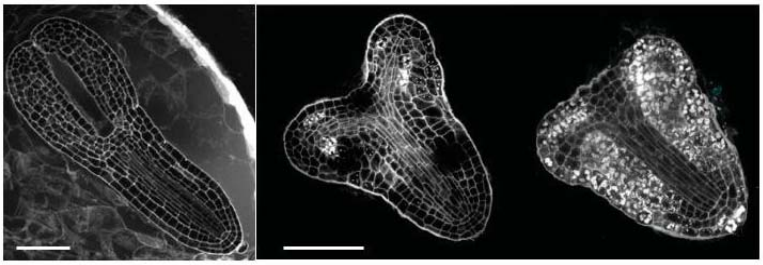

Supplemental Figure 4. Morphology of *pas1-3* embryos at late torpedo stage showing intermediate phenotype with the development of cotyledon structures, which will never expand (middle and right). Wild-type embryo from *pas1*/+silique at the same stage is shown left. Starch could be observed as white dense cellular material stained with propidium iodide. Note starch staining in *pas1-3* cotyledon (arrow head). Bar, 40 μm

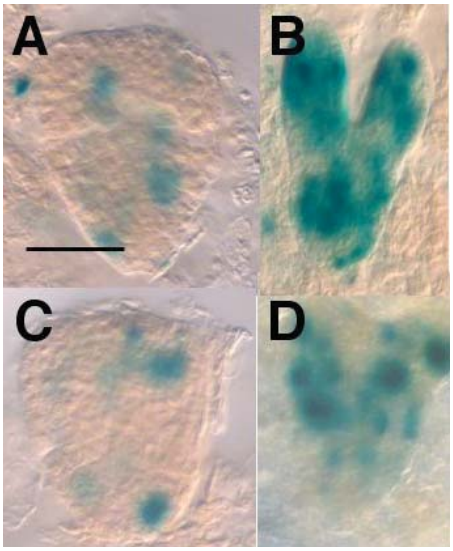

Supplemental Figure 5. Cell division pattern is not modified in *pas1-3* mutant.
Expression of the mitotic marker *pCycB1;1:db-GUS* was monitored in wild-type (A-B) and *pas1-3* (C-D) embryos. The pCycB1;1:db-GUS expression was analyzed at two different developmental stages: heart (A and C) and torpedo (B-D) stages. *pas1-3* and wild-type embryos were isolated from the same *pas1-3*/+ silique. Bar, 40 μm

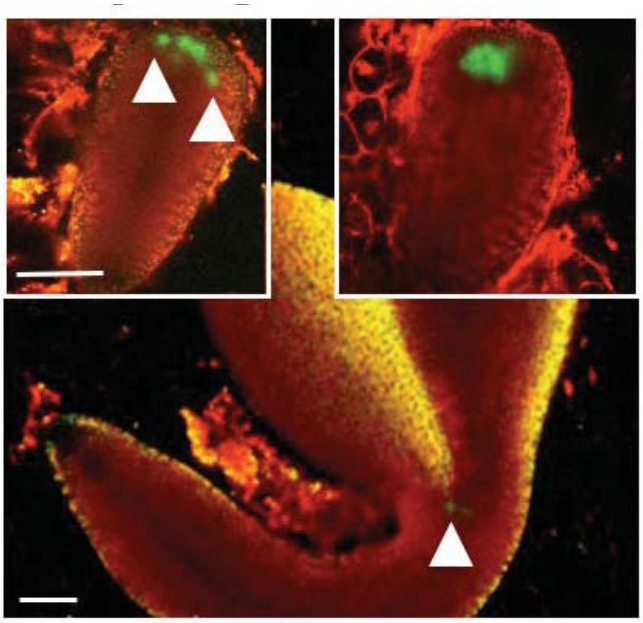

Supplemental Figure 6. The *WUS* domain is larger in *pas1-3*.
pWUS:GFP expression was monitored in wild-type (bottom) and mutant (top) embryos. WUS expression domain is enlarged and scattered in several non-adjacent cells (arrows) in *pas1-3* embryos as opposed to wild-type (arrows). The embryos are at the same developmental stage. Bar, 40 μm

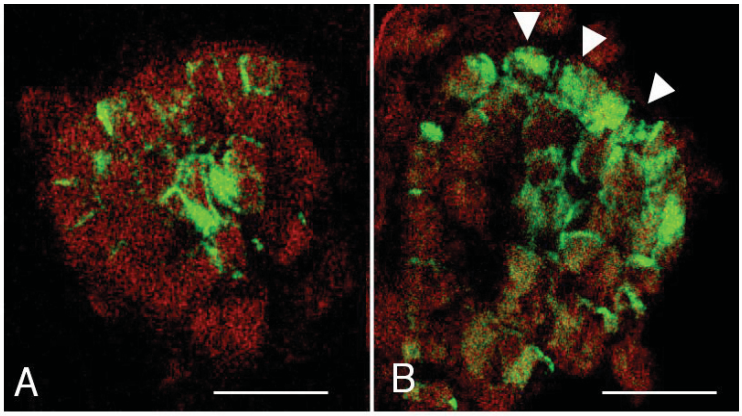

Supplemental Figure 7. Altered PIN1 distribution in *pas1-3*/+ embryos at late globular - early heart stage.
PIN1 immulocalization was performed on late globular embryos from segregating *pas1*/+ silique. At this stage, wild-type and *pas1-3* embryos do not show a significant phenotypic difference but segregating embryos based on their PIN1 distribution in apical cells could be observed. Some embryos showed clear aggregation and unpolar distribution of PIN1 (B, arrows) while the majority of the embryos showed polar distribution of PIN1 (A). Bar, 10 μm.

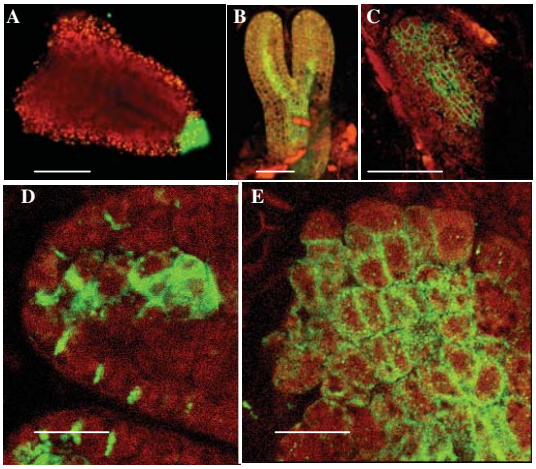

Supplemental Figure 8. Auxin accumulation and PIN1 polar distribution are altered in *pas3* embryo.
(A) *pDR5:GFP* expression in *pas3-1* mutant.
(B-E) Immunolocalization of PIN1. Comparison of PIN1 distribution between wild-type (B) and *pas3-1* mutant (C). Detail of PIN1 distribution in the tip of a wild-type cotyledon (D) and *pas3-1* embryo apex (E).
Bars, 40 μm (A, B, H); 20 μm (C, I); 10 μm (D,E); 2 mm (F), 5 μm (G).

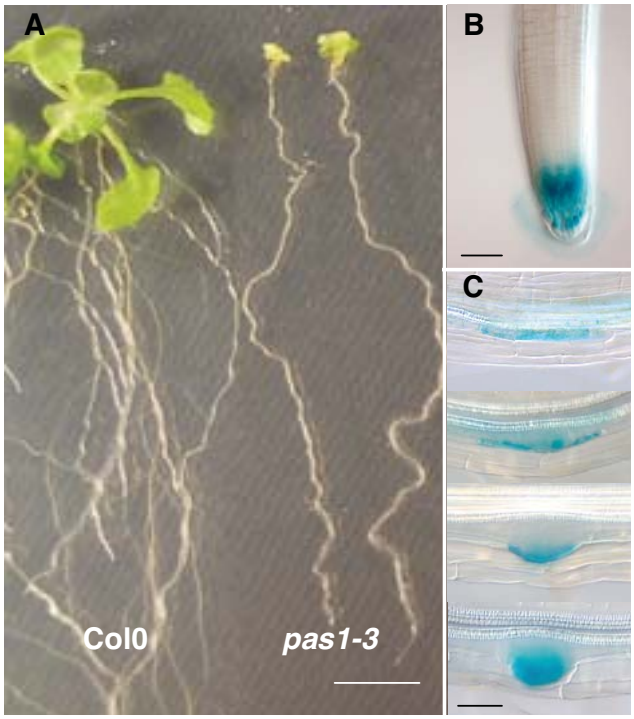

Supplemental Figure 9. PAS1 is involved in lateral root development.
(A) Lateral root development is inhibited in *pas1-3* mutant. Bar, 5 mm.
(B) *pPAS1:GUS* expression in wild type primary root is restricted to the meristem and the columella cells. Bar, 70 μm.
(C) *pPAS1:GUS* expression during lateral root initiation in wild type seedlings. Different stage of lateral root development are shown from the first pericycle divisions (top) to root outgrowth (bottom). Bar, 40 μm.

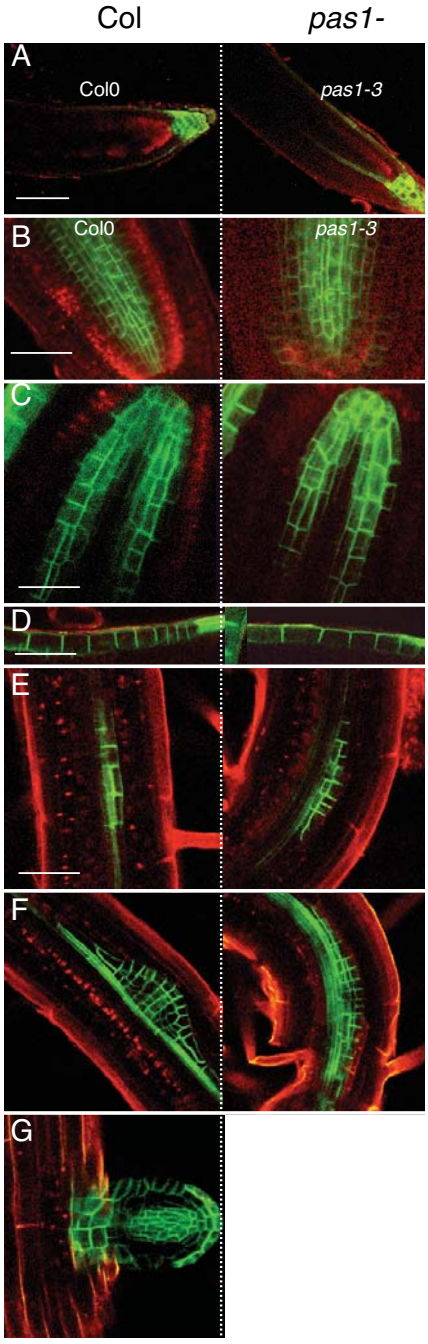

Supplemental Figure 10. Polar auxin transport during *pas1* root development.

(A) *pDR5:GFP* expression in wild-type (left) and *pas1-3* in primary root (right).

(B) *pPIN1:PIN1-GFP* expression in wild-type (left) and *pas1-3* in primary root (right)

(C) *pAUX1:AUX1-YFP* expression in primary root protophloem (in wild-type (left) and *pas1-3* in primary root (right).

(D) *pAUX1:AUX1-YFP* expression in primary root epidermis (in wild-type (left) and *pas1-3* in primary root (right).

(E-G) *pAUX1:AUX1-YFP* expression during lateral root development in wild-type (left) and *pas1-3* in primary root (right). The *pas1-3* mutant never showed any lateral root outgrowth like observed in wild type (G)

Bars, 70 μm (A); 45 μm (B); 20 μm (C, D); 45 μm (E - G).

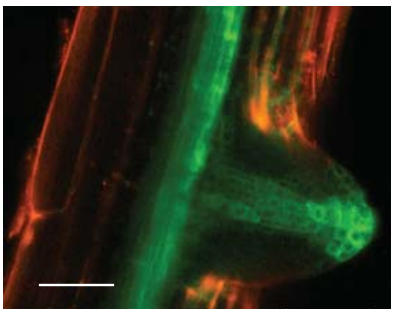

Supplemental Figure 11. *pDR5:GFP* expression in emerging lateral root of wild-type seedlings . Bar is 35 μm.

Supplemental Table 1. Relative sterol and sterol glycoside levels in *pas1* and *pas3* mutants

	Col 0	*pas1-3*	*pas3-1*
Sterols	10.8 ± 1.1 (n=5)	16.1 ± 1.9 (n=5)	14.2 ± 1.8 (n=3)
Sterol-glycosides	5.2 ± 1.1 (n=5)	5.4 ± 1.9 (n=5)	6.4 ± 1.8 (n=3)

Sterols and Sterol-glycosides are expressed as % of total lipid mass. Each value is the mean of several experiments (n) ±SEM.